

Self-Calibration of Redundantly Actuated PKM exploiting Kinematic Landmarks

Andreas Müller and Maurizio Ruggiu

Abstract A self-calibration method for redundantly actuated parallel manipulators (RA-PKM) is proposed that uses motion reversal points (MRP) of actuators as kinematic calibration landmarks. The basic principle is to restrain a RA-PKM to 1 DOF and detect the MRP of redundant actuators. The difference of measured MRP and those deduced from a kinematic model embodies the calibration error. Therewith a numerical adaptation scheme is introduced. Simulation results for a 3 DOF RA-PKM confirm very high accuracy of the method.

Key words: Calibration, parallel manipulators, redundant actuation, singularities

1 Introduction

Kinematic calibration of robotic manipulators is commonly based on the acquisition of redundant measurement data [4, 10, 13, 14]. Actuator readings are compared with external end-effector (EE) measurements. The need for external measurement devices makes the calibration expensive and prohibits simple repetition. Moreover, due to the external measurements, traditionally calibration methods are inherently intrusive. In order to alleviate this intrusion several authors [1, 5, 12, 15, 17] proposed to acquire redundant measurements by locking selected joints of a parallel kinematics machine (PKM). Other schemes aiming at semiautonomous calibration are reported in [16] and [20] where some passive joints are equipped with sensors providing redundant sensor data without application of external devices. A fully autonomous self-calibration method should not require additional sensors, externally or at passive joints. An important observation is that redundant actuation implies sensor redundancy since it does not increase the DOF of a PKM but gives rise to more encoder readings than necessary to position the PKM. It thus allows for application

Andreas Müller, Inst. of Mechatronics, Chemnitz, Germany, andreas.mueller@ifm-chemnitz.de
Maurizio Ruggiu, Dep. Mech. Eng., University Cagliari, Italy, ruggiu@dimeca.unica.it

of the traditional calibration methods as pursued in [18]. Other tailored calibration methods were reported in [2, 19] exploiting the tracking error projected to the null-space of the forward kinematics Jacobian. In this paper a calibration method is proposed that follows a completely different approach. Instead of comparing redundant sensor data the occurrence of kinematic landmarks is compared and exploited for adaptation of the geometric machine parameters. These landmarks are detected inherently by means of actuator measurements. The redundancy required for calibration is thus achieved by the actuation redundancy. The simulations reveal a high accuracy of the method. Throughout the paper configurations where the velocity of one actuator becomes zero, while the EE performs continuous motion, will be called **motion reversal points** (MRP) of that actuator. δ denotes the manipulator's DOF. The vector summarizing the geometric model parameters is denoted $\pi \in \Pi$ where Π is a p -dimensional parameter space manifold.

2 Main Principle: Motion Reversal Points

Undoubtedly kinematic singularities are significant kinematic landmarks intrinsically related to the PKM geometry, and it shall be expected that this can be exploited for the calibration purpose. A singularity-based calibration method was proposed for a non-redundant planar 3-DOF PKM [6, 7, 8], and later applied [11] to the calibration of a non-redundant spatial 3PRS PKM. The basic idea of that method is to detect active input singularities [3] in the plant by measurements in the actuated joints as well as in a parameterized kinematic model, and to adapt the geometric parameters so that these singularities coincide. Active singularities are characterized by a reversing motion, i.e. a zero velocity, of some actuator coordinates for a continuous EE-motion. This allows to detect them without additional sensors.

The calibration scheme proposed in [6, 7, 8, 11] was originally developed for non-redundantly actuated PKM. This poses the apparent problem that the PKM must be steered into a critical configuration in which it is not fully restrained by means of the actuators, and cannot be controlled safely. Moreover in these situations the actuator may mutually interfere. To cope with this problem and ensure passage through the singularity, in [6, 7, 8] the PKM was given an initial motion so to passively swing through the input singularity, enabling detection of the reversing motion of one of the actuators. In order to actually detect these singularities the PKM's mobility must be restrained, which is apparent observing that singularities form lower dimensional subvarieties in the configuration space (c-space) that almost sure will not be hit when the PKM can move freely in the c-space. To this end in [6, 7, 8] the mobility was reduced to 1 DOF by deactivating the one (backdrivable) actuator for which a MRP (i.e. a zero crossing of its velocity) is to be detected, and locking all remaining $\delta - 1$ actuators. Then only motions of the deactivated (backdrivable) actuator are possible, and the problem of detecting the input singularities of that particular actuator reduces to a one-dimensional problem. Clearly then the non-redundantly actuated PKM is not controllable anymore

since the only one movable actuator is passive. It was proposed to let the PKM passively swing through the anticipated singularity. In Fig. 1 actuators 1 and 3 could be locked and the MRP of the released actuator 2 be observed when the PKM is set in motion. The locked actuators 1 and 3 (with fixed lengths) together with the platform constitute a planar 4-bar linkage. The mount point of actuator 2 moves on the coupler curve of that 4-bar, and a MRP occurs when the point reaches the point on that curve that is closest to the mount point on the base. This configuration is indicated in Fig. 1 by a dashed line. Such passive motion requires external stimulus and precaution. Redundant actuation allows to exploit this principle in a safe and reliable way. The crucial point is that MRP can also be observed in RA-PKM but without meeting input singularities, i.e. without entering critical poses.

Input-singularities of a non-redundantly actuated PKM with DOF δ can be eliminated by introducing $m > \delta$ actuators, of which $\rho = m - \delta$ are redundant that can always control the PKM. Consequently, actuation redundancy allows controlling the RA-PKM through points that are input-singularities of the non-redundant PKM, i.e. when controlled by some δ out of the m actuators. Since MRP are significant points, that are inherently related to the mechanism geometry, they can be considered as kinematic **calibration landmarks**. This is the basis for a self-calibration method introduced in [9] where the feasibility was demonstrated by application of an ad hoc

minimization algorithm. In this paper the method is completed by a computationally efficient update algorithm. The redundantly actuated 4RPR in Fig. 2a) (3RPR with an added fourth actuated chain is used as example. The joints are mounted at the corners of a rectangle. The RA-PKM still has $\delta = 3$ DOF but is actuated by $m = 4$ prismatic actuators. Also for this RA-PKM joint 2 exhibits MRP, but now, due to the actuation redundancy, the manipulator can safely be controlled through these MRP as shown in Fig. 2a). After locking $\delta - 1 = 2$ actuators there are still $m - \delta + 1 = 2$ actuators left of which one is that for which MRP are sought and the other one can be used to drive the (1-DOF) system. Actuators 1 and 4 can be locked and actuator 3 be used to move the manipulator while observing the MRP of actuator 2. A deviation of the geometric parameters from the actual plant geometry is reflected by MRP occurring at different locations. Minimizing this difference is a means for model calibration. This was pursued in [9] where the calibration error was defined as the squared difference of MRP analytically computed from the kinematic model and MRP detected in the plant for N different measurements. For example in Fig. 2b) this error would be $e := \sum_{i=1}^N (\hat{\theta}_0^{2,i} - \theta_0^{2,i})^2$ where $\theta_0^{2,i}$ is the MRP of actuator joint 2 deduced from the model, and $\hat{\theta}_0^{2,i}$ is the corresponding MRP detected in the plant for the i th measurement. The critical point when directly minimizing e is that this is a non-linear problem and that it requires an analytic expression for the MRP.

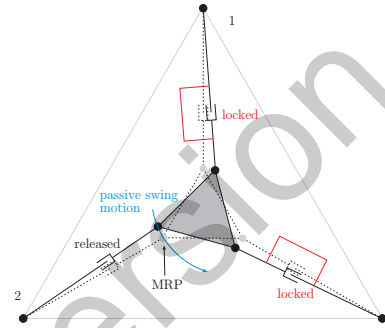


Fig. 1 MRP detection of a 3RPR manipulator via a passive swing motion. Actuators 1 and 2 are locked and 3 is free to move passively.

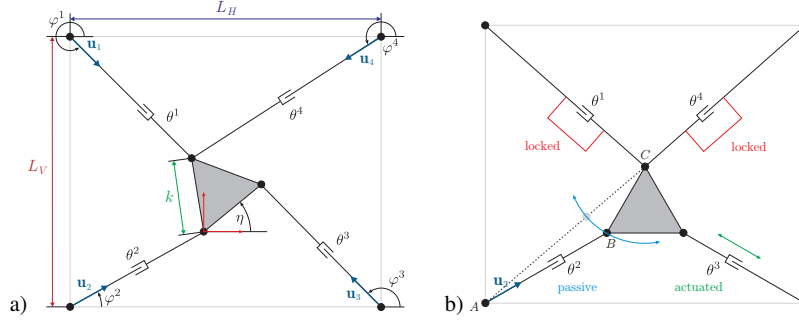


Fig. 2 a) Planar 3-DOF 4RPR RA-PKM. b) Detection of MRP of actuator 2. Actuators 1 and 4 are locked, and 3 is actuated. The MRP occurs when point B is closest to point A, as indicated.

Here a MRP-based calibration method is introduced that does not suffer from these restrictions. For RA-PKM with actuation redundancy $\rho = m - \delta$ it consists of three constituent parts: 1) the restriction of the RA-PKM mobility to 1 DOF by locking $\delta - 1$ actuators, 2) detection of MRP, and 3) model adaptation.

3 Selection of Locked Actuators

The RA-PKM is restrained to 1-DOF motions by locking $\delta - 1$ actuators. This leaves a manipulator with $m - \delta + 1$ movable actuators. Out of these one actuator is used to drive the restrained RA-PKM. The remaining $\rho = m - \delta$ actuators are deactivated and presumed to be backdrivable. Since actuators are equipped with encoders the MRP of these ρ joints can be detected by controlling the 1-DOF motion. The choice of locked actuators is not unique. In general there are $C_{\delta-1}^m = \binom{m}{\delta-1}$ different possibilities to lock $\delta - 1$ of the m actuators. Most RA-PKM reported in the literature possess simple actuation redundancy, i.e. $m = \delta + 1$, $\rho = 1$, and this assumed in the following. Then $\delta - 1 = m - 2$ actuators must be locked, for which there are $C_{m-2}^m = \frac{(m-1)m}{2}$ different possibilities. Fixing $\delta - 1$ actuators leaves two unlocked. One of these two can be controlled so to detect the MRP of the other one. In this way, for each one of the C_{m-2}^m combinations, the MRP of one deactivated actuator can be detected. For each combination of locked actuators there are two possible actuation schemes. In total there are $2C_{m-2}^m$ different actuation schemes for detecting MRP (generally $(\rho + 1)C_{\delta-1}^m$).

Denote $\theta = (\theta^1, \dots, \theta^m)$ the vector of actuator coordinates. For each of the C_{m-2}^m possibilities denote with $\theta_l, l = 1, \dots, C_{m-2}^m$ the vector of the $\delta - 1$ locked actuator coordinates. The remaining two **free actuator** coordinates are denoted with θ^j and θ^i , where j refers to the controlled and i to the free passive actuator for which the MRP is sought. The coordinate vector θ is thus partitioned into θ_l, θ^j and θ^i . In Fig. 2b) it is $\theta_l = (\theta^1, \theta^4)$, $\theta^j = \theta^3$, and $\theta^i = \theta^2$.

4 Detection of MRP

For a specified set l of locked actuators, the detection of MRP of θ^i in the model requires an **indicator function**, denoted with F_{ij}^l , such that $F_{ij}^l = 0$ if and only if $\dot{\theta}^i = 0$ for any $\dot{\theta}^j$. The condition $F_{ij}^l = 0$ allows inferring the joint coordinate θ_0^j of the controlled actuator where MRP of the free passive actuator i occurs in the model for given θ_i and geometry π . An obvious candidate for such an indicator function is the velocity inverse kinematics solution for actuator i (sec. 6). The MRP of actuator joint i deduced from the model is denoted θ_0^i . In Fig. 2b) the indicator function F_{23} returns the velocity of joint 2 when the manipulator is driven by actuator 3 with the remaining joints 1 and 4 locked. The MRP in the plant are detected monitoring the sign of the velocity of the free passive actuator i while performing a smooth 1-DOF motion controlled by actuator j . The detected MRP are only exact up to the measuring accuracy/encoder resolution, and denoted $\hat{\theta}_0^i$.

5 Calibration Algorithm

The model adaptation exploits the difference of MRP predicted in the model and those measured in the plant. By locking different sets of $\delta - 1$ actuators the MRP can be detected for all m actuators. For a particular set of locked actuators, indexed with l , the remaining two actuator coordinates are interchangeably used to drive the 1-DOF system. This detection is repeated at N different points in the c-space, i.e. for different values of θ_l giving rise to an input data set for the calibration.

The strategy is to detect the MRP of actuator i for a set of locked actuators. Crucial for the calibration algorithm is the indicator function. It is thus desirable to have an indicator function that only depends on θ^i and θ_l , which represent δ non-redundant actuator coordinates. But, depending on the complexity of the kinematics, it may not possible to analytically construct such an indicator function. These cases are distinguished in the following. The PKM pose is locally uniquely determined by δ actuator coordinates, and in particular by the actuator coordinates θ^i and θ_l . Now by definition this unique dependence ceases at the MRP of actuator i . In the 4RPR example in Fig. 2b) the motion is determined by θ^1, θ^4 , and θ^2 except at the MRP of joint 2. Nevertheless, presumed that the closed loop constraints can be expressed in terms of these δ actuator coordinates, it can be assumed that the indicator function attains the form $F_{ij}^l(\theta^i, \theta_l; \pi)$. That is, F does not depend on the controlled actuator coordinate θ^j nor on any coordinates of passive joints. Let $\hat{\theta}_0^i = \theta_0^i + \Delta\theta_0^i$ be the measured joint coordinate of the passive actuator i where its MRP occurs. $\Delta\theta_0^i$ represents the deviation from the joint coordinate θ_0 where MRP occurs in the model. Denote with

$$\pi = \pi_0 + \Delta\pi \quad (1)$$

the (unknown) geometric parameters of the plant. Here π_0 is the nominal geometry used as initial value in the model, $\Delta\pi$ is the geometric imperfection to be estimated.

Evaluating the indicator function with the measured MRP values and the nominal model parameters will yield $F_{ij}^l(\hat{\theta}_0^i, \theta_l, \pi_0) \neq 0$. That is, using the nominal model parameters, the analytic indicator function would not detect the MRP. Moreover, the value of F_{ij}^l does represent a **calibration error**. This error is minimized adapting π_0 .

Since the locked actuator coordinates θ_l are input to model and plant the only information about model uncertainties are conveyed by $\hat{\theta}_0^i$. Hence, treating $\Delta\theta_0^i$ and $\Delta\pi$ as variables, and neglecting measurement errors, leads to the first-order condition

$$F_{ij}^l(\hat{\theta}_0^i, \theta_l, \pi_0) - \frac{\partial F_{ij}^l}{\partial \theta^i} \Delta\theta_0^i + \frac{\partial F_{ij}^l}{\partial \pi} \Delta\pi = 0. \quad (2)$$

The measurement is repeated at N_l different locations of MRP of θ^i giving rise to an overdetermined linear system

$$\begin{pmatrix} \frac{\partial F_{ij}^l}{\partial \theta^i} \Delta\theta_{0,1}^i - F_{ij}^l(\hat{\theta}_{0,1}^i, \hat{\theta}_{l,1}, \pi_0) \\ \frac{\partial F_{ij}^l}{\partial \theta^i} \Delta\theta_{0,2}^i - F_{ij}^l(\hat{\theta}_{0,2}^i, \hat{\theta}_{l,2}, \pi_0) \\ \vdots \\ \frac{\partial F_{ij}^l}{\partial \theta^i} \Delta\theta_{0,N_l}^i - F_{ij}^l(\hat{\theta}_{0,N_l}^i, \hat{\theta}_{l,N_l}, \pi_0) \end{pmatrix} = \begin{pmatrix} \frac{\partial F_{ij}^l}{\partial \pi} \\ \frac{\partial F_{ij}^l}{\partial \pi} \\ \vdots \\ \frac{\partial F_{ij}^l}{\partial \pi} \end{pmatrix} \Delta\pi \quad (3)$$

written as $\mathbf{y}_l = \mathbf{M}_l \Delta\pi$, where the partial derivatives of F_{ij}^l are evaluated at $\hat{\theta}_{0,k}^i, \theta_{l,k}$, $\pi_0, k = 1, \dots, N_l$. The values of $\Delta\theta_{0,k}^i = \hat{\theta}_{0,k}^i - \theta_{0,k}^i$ are computed from the difference of measured values and those deduced from the model. For p parameters \mathbf{M}_l is a $N_l \times p$ matrix. This measurement procedure can be carried out for different choices of locked actuators indicated by the subscript l , for which there are $2C_{m-2}^m$ options. It is usually not necessary to exhaust all these combinations, however. Denote with \mathbf{M} the $N \times p$ matrix comprising the \mathbf{M}_l submatrices, and with \mathbf{y} the corresponding left-hand side vector of length N . The system (3) is solved via a pseudoinverse of \mathbf{M} as $\Delta\pi = (\mathbf{M}^T \mathbf{M})^{-1} \mathbf{M}^T \mathbf{y}$. The final update for the parameter vector is $\pi = \pi_0 + \Delta\pi$. The solution π of the linear approximation (2) may not lead to a vanishing F_{ij}^l . Therefore the adaptation step is repeated. Denoting with π_v the obtained parameter values at step $v = 1, 2, \dots$ then an improved estimate π_{v+1} is found by application of the above update step with π_v as initial parameter. The calibration starts with π_0 .

6 Simulation Example

The planar 3 DOF 4RPR RA-PKM in Fig. 2a) has $m = 4$ of actuators and actuation redundancy $\rho = 1$. The moving platform forms an equilateral triangle with side lengths k . The mount points on the ground are located at the corners of a rectangle with side lengths L_H and L_V . The reference displacements of actuators 1 and 4 for $\theta^1 = \theta^4 = 0$ is denoted with L_1 and L_4 . The parameter vector is $\pi = (L_1, L_4, L_H, L_V, k)$. The nominal parameter values are $\pi_0 = (0, 0, 0.5, 0.5, 0.15)$ m.

Numerical results are reported using MRP of actuators 2 and 3 when joints 1 and 4 are locked. That is, only one set of locked actuators is used, for which the MRP of joint 2 is determined when controlled by actuator 3, and the MRP of joint 3 is determined when controlled by actuator 2. The calibration performance is examined for two sets of calibration points in Fig. 3. During calibration actuators θ_1, θ_4 are positioned and locked so that actuator 2 of the model with nominal parameters π_0 exhibits a MRP when point B of the platform coincides with the calibration point (Fig.

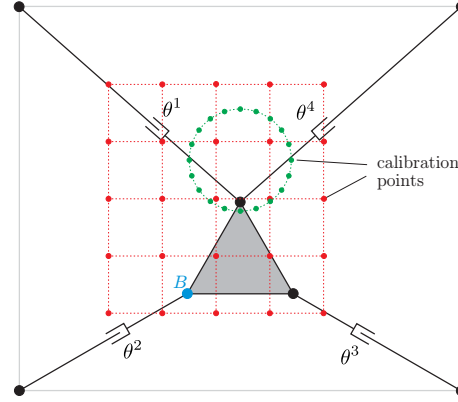


Fig. 3 Calibration points on a grid and on a circle in workspace.

3). The first set consists of 4×4 samples on an equidistant grid. The second set comprises 20 points uniformly distributed on a circle. The plant parameters are randomly set to $\pi = \pi_0 + (\Delta L, -\Delta L, -\Delta L, -\Delta L, +\Delta L)$ with a deviation of $\Delta L = 10^{-3}$ m and $\pi_0 = (0, 0, 0.5, 0.5, 0.15)$ m. Simulating encoder precision the joint measurements in the plant are quantized with encoder resolution Δx . Fig. 4a) shows the evolution of calibration error for perfect measurement (no measurement errors), and for quantizations $\Delta x = 10^{-4}$ and $\Delta x = 10^{-3}$, when 16 calibration points on the grid in Fig. 2b) are used. Shown is the mean value of the absolute deviation of the model from the plant parameters after step i . After 3 steps the calibration converges to the computation accuracy if joint angles are measured perfectly. Otherwise the convergence is bounded by the quantization Δx . For the chosen quantization convergence is observed after one iteration. The final calibration error is below the uncertainty Δx , which can be explained as an averaging effect. Similar results are found for the 20 calibration points on the circle in Fig. 4b).

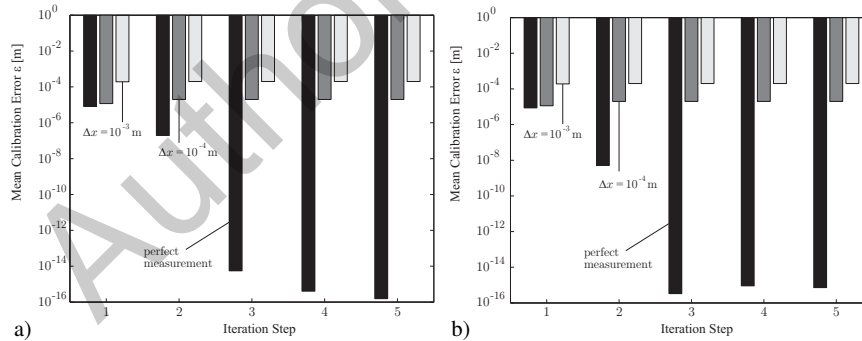


Fig. 4 a) Calibration error evolution for different measurement accuracies Δx a) using 16 calibration points on a grid in Fig. 3 b) 20 calibration points on the circle in Fig. 3 ($\Delta L = 10^{-3}$).

7 Conclusions and Outlook

A self-calibration method for RA-PKM has been proposed based on motion reversal points. The method does not require any additional sensors. The only (but possibly critical) condition on RA-PKM is that the drives for which MRP are detected must be backdrivable. The general concept is introduced and numerical results are shown for a simple 3 DOF planar RA-PKM. For this example the method shows very good performance and accuracy. Future work will address the sensitivity and convergence of algorithm in order to develop a calibration planning strategy.

References

1. D.J. Bennett, J.M. Hollerbach: Autonomous Calibration of a Single Loop Closed Kinematic Chain formed by Manipulators with Passive Endpoint Constraints, *IEEE T.Rob.Aut.*, 7(5)1989
2. S. Cong et al.: Kinematic Parameters Auto-Calibration of Redundant Planar 2-Dof Parallel Manipulator, *Parallel Manipulators, New Developments*, I-Tech Publishing, Vienna, 2008
3. C. Gosselin, J. Angeles: Singularity analysis of closed loop kinematic chains, *IEEE Trans. Rob. Automat.*, 6(3) 1990
4. J. M. Hollerbach, C. W. Wampler: The Calibration Index and Taxonomy for Robot Kinematic Calibration Methods, *Int. J. Rob. Res.*, 15(6) 1996
5. W. Khalil, S. Besnard: Self-calibration of Stewart-Gough parallel robots without extra sensors, *IEEE Trans. Rob. Autom.*, 15(6) 1999
6. P. Last, C. Budde, J. Hesselbach: Self-Calibration of the HEXA-Parallel-Structure, *Proc. IEEE Int. Conf. Aut. Science and Eng. (CASE)*, August 1-2, 2005, Edmonton, Canada
7. P. Last, D. Schütz, A. Raatz, J. Hesselbach: Singularity Based Calibration of 3-DOF Fully Parallel Planar Manipulators. 12th IFToMM World Cong., Besancon, France, June 18-21, 2007
8. P. Last, A. Raatz, J. Hesselbach: Singularity-Based Calibration - A Novel Approach for Absolute-Accuracy Enhancement of Parallel Robots, in A. Lazinica, H. Kawai (Ed.): *Robot Manipulators New Achievements*, 2010, InTech Publishing
9. A. Müller, M. Ruggiu: Self-Calibration of Redundantly Actuated PKM based on Motion Reversal Points, in J. Lenarcic, M. Husty (ed.): *Latest Adv. in Robot Kinematics (ARK) 2012*
10. A. Nahvi, J. M. Hollerbach, V. Hayward: Calibration of parallel robot using multiple kinematic closed loops, *IEEE ICRA*, 1994
11. S.M. O'Brien, J.A. Carretero. P. Last: Self Calibration of 3-PRS Manipulator Without Redundant Sensors, *Transactions of the Canadian Society for Mechanical Engineering*, 31(4) 2007
12. H. Ota, et. al: Forward kinematic calibration method for parallel mechanism using pose data measured by a double ball bar system, *Int. Conf. Parallel Kin. Mach.*, 2000
13. A. Rauf, S.G. Kim, J. Ryu: Complete parameter identification of parallel manipulators with partial pose information using a new measurement device, *Robotica*, 22(6) 2004
14. A. Rauf, A. Pervez, J. Ryu: Experimental Results on Kinematic Calibration of Parallel Manipulators Using a Partial Pose Measurement Device, *IEEE Trans. Rob. Control*, 22(2) 2006
15. J. Ryu, A. Rauf: A new method for fully autonomous calibration of parallel manipulators using a constraint link, *IEEE/ASME Int.Conf.Adv.Intel.Mech. (AIM)*, Como, Italy, July 8-12,2001
16. C. W. Wampler, J. M. Hollerbach, T. Arai: An implicit loop method for kinematic calibration and its application to closed-chain mechanisms, *IEEE Trans. Robot. Autom.*, 11(5) 1995
17. M. Weck, D. Staimer: Accuracy Issues of Parallel Kinematic Machine Tools: Compensation & Calibration, *Int. Conf. Paral. Kin. Mach.*, 2000
18. Y.K. Yiu, J. Meng, Z.X. Li: Auto-Calibration for a Parallel Manipulator with Sensor Redundancy, *Proc. IEEE Int. Conf. Rob. Automat. (ICRA)*, Sept. 14-19, 2003, Taipei, pp. 3660-3665
19. Y.X. Zhang, S. Cong, W.W. Shang, Z.X. Li, S.L. Jiang: Modeling, Identification and Control of a Redundant Planar 2-DOF Parallel Manipulator, *Int. J. Control, Aut. Sys.*, 5(5) 2007
20. H. Zhuang: Self-Calibration of Parallel Mechanisms with a Case Study on Stewart Platforms, *IEEE Trans. Rob. Autom.*, 13(3) 1995